Journal of Electrical Engineering and Computer (JEECOM)
Vol. 7, No. 2 (2025), DOI: 10.33650/jeecom.v4i2
p-ISSN: 2715-0410; e-ISSN: 2715-6427

Monitoring Design on PV and Battery PLTS for Power Regulation on Water Pump

Sri Sukamta [1], Ulfah Mediaty Arief [2], M.Hendri Akbar Daffa[3], Banu Mahmuda Hafids[4], Shindi Aulia Nidha[5], Anisa Susilawati[6], Ade Yusuf[7], Juniar Ibrahim[8]
[1,2,3,4,5,6,7,8] Department of Electrical Engineering, Universitas Negeri Semarang, Semarang, Indonesia

Article Info

Article history:

Received Juny 9, 2025
Revised July 14, 2025
Accepted Sept 26, 2025

Keywords:

Power Monitoring
Battery
Photovoltaic
Water Pump
Power Regulation

ABSTRACT

The increasing use of solar energy as a source of electrical energy encourages the use of remote monitoring systems to determine the performance of solar panels. The purpose of this study is to conduct a monitoring system for solar panel (PV) and battery output for water pump loads. The method used is to design a monitoring system using the microcontroller NodeMCU ESP8266 and sensor INA219. The first step is to determine the capacity of the PV, battery, and water pump. Then do microcontroller programming and field testing. The INA219 sensor measures the operating voltage and current in real time, the voltage, power, and current of the PV connected to the circuit. Experimental investigations that have been carried out to verify the effectiveness of the proposed monitoring system have shown that proper examination of the collected data allows the monitoring system to be enlarged. The monitoring system is able to perform measurements well for 3 months. The results of monitoring measurements in this study are also influenced by the intensity of solar radiation.

Corresponding Author:
Sri Sukamta,
Universitas Negeri Semarang, Sekaran Gunung Pati, Semarang and 50229, Indonesia
Email: ssukamta2014@gmail.unnes.ac.id

1. INTRODUCTION

Photovoltaic (PV) systems have been widely used in residential areas to reduce energy costs. However, these systems are not monitored in detail or managed in a user-friendly manner in many cases. Therefore, a PV monitoring system needs to provide detailed monitoring for each PV module and an easy-to-use way to access the monitored data. In addition, the PV monitoring system must be low-cost to be widely used [1]. The integration of renewable energy (RE) resources into the power system poses many research challenges. Studies have shown that RE output can exceed the power consumed during the day. As a result, the direction of power flow in the distribution network can be reversed for some periods. Since voltage controllers are usually designed for unidirectional power flow, this can cause voltage differences at the distribution center. In addition, the intermittent and non-distributable installation of photovoltaic (PV) devices increases the control problem of the distribution system. Intelligent photovoltaic (PV) module monitoring can automatically locate the panel position and monitor the status of the PV module, which is very important for the operation and maintenance of solar power plants. As a new communication method in the field of PV monitoring, PV module monitoring based on power grid communication is the future trend of solar power plant monitoring due to its low maintenance cost and strong anti-interference ability [2].

Further research on PV monitoring was conducted by authors [3], proposing an intelligent PV module monitoring scheme based on parallel resonant coupling unit, which uses DC bus as communication channel and modulates monitoring data into high frequency form to perform carrier communication. Experimental results achieved by the developed grid transceiver demonstrate the feasibility and validity of the proposed scheme. Aluminum electrolytic capacitors (AEC) are used in the DC-link of a grid-connected single-phase solar inverter to suppress DC-link voltage oscillations. Furthermore, long-term use of capacitors can cause open circuits in the dc-link. A quasi-online method for monitoring AEC conditions in solar inverters is

ISSN: 2715-6427

proposed [4], [5]. This method is active at night when there is no solar radiation. The main advantage of this technique is that it combines energy and capacitance estimation to determine monitoring. Furthermore, this technique does not require significant processing power and is implemented in existing digital processors/controllers used for inverter control. In this study [6], [7] an innovative sensor is proposed that is suitable for measuring the operating voltage and current, open circuit voltage, and short circuit current of connected PV in real-time. An effective disconnection system ensures that the sensor does not affect the circuit characteristics during the measurement phase and offers many benefits. Extensive experiments were carried out to prove the reliability and usefulness of the sensor for continuous monitoring of PV power plants. As the deployment rate of PV power plants continues to increase, the need for a good and scalable method for performance analysis increases. Therefore, an approach to measure the quality level of utility-scale PV power plants is proposed [8]. This method is validated on data from three utility-scale PV power plants that produce loss rates in the range of 0%-0.18%/day. Next, a method for monitoring aluminum electrolytic capacitors (AEC) using the measured parameters for maximum power point tracking is proposed [9]. While the method [10] proposes real-time detection of series resistance changes in PV modules. The proposed technique is for continuous/discontinuous conduction modes in converter operation. Simulation studies are carried out and the results are in accordance with those obtained. Proper monitoring, operation and maintenance of PV systems are part of the service tasks required to ensure long-term reliability and longer installation life [11]. This method describes a remote monitoring technique that can be used for general standardization and as a common basis for effective reliability assessment, monitoring, operation and maintenance. The next study conducted a PV arrangement based on wireless radio frequency identification (RFID) technology. In this design, up to seven digital humidity sensors are used soldered on 130 μm thick polyimide foil that also integrates the necessary RFID antennas and readouts. Its very small size and wireless design allow its placement anywhere in the PV module either in front or on the back side of the solar cell. This system is applied in a mini module with a single full-size crystalline silicon solar cell and exposed to high temperature and humidity conditions. Authors [12] provide an overview of safety enhancement technologies in battery management, while authors [13]. Proposed a battery management system (BMS) used during the operation of electric vehicles (EVs) to monitor, predict, and control the battery status to ensure that the battery can function effectively and safely. In addition, the material composition, system design, and operating conditions substantially affect the battery life, making it more challenging to manage and maintain the battery system.

Multifrequency impedance measurement has been known as a technique for monitoring cells in lithium-ion (Li-ion) batteries. However, battery management is slow, mainly due to its larger size and higher operating power requirements. Therefore, a small and low-power multifrequency (1-1000 Hz) impedance-based battery management system (BMS) for multi-cell batteries with various capacities is proposed. This BMS ensures battery safety and efficiency by tracking and acting on the emerging mismatches and other electrical and thermal abnormalities in each individual cell without increasing the cost, volume, weight, and power, compared to conventional BMS. In order to eliminate the faults of lithium-ion batteries and improve the user level, a control method for the energy balance of lithium-ion batteries is proposed for the Internet of Things [14]–[16]. Experiments show that this method can effectively control the energy balance of lithium-ion batteries, when the experiment reaches 50 seconds, the final time of lithium battery balance control is about 540 seconds, the balance efficiency is greater than 98%. Battery Management System performs various tasks, including monitoring voltage and current, estimating charge and discharge, equalizing and protecting the battery, managing temperature conditions, and managing battery data [17]. Electrical energy from the utility grid is still typically used when submersible pumps are used. PV can be utilized as a source of electrical energy if the submersible pump is situated in an area that is accessible to the utility grid. This article's goal is to create a microgrid system that uses a PV source and batteries to power submersible pumps in rural regions. Furthermore, a PV and grid power regulation by performing load monitoring is proposed [18], [19]. 10 PV 100 Wp, 1500 Ah batteries, and SCC 150 A are required to construct this system. According to the study's findings, 2,796 kWh of electrical energy are used in a single day, meaning that the average monthly electrical energy consumption is 83.88 kWh, while 3,473 kWh of PV energy is produced. PV energy and batteries can be used to supply load energy. In addition, the grid energy source serves as a backup and is employed in the event that the PV source or battery is disconnected, whereas the logic controller can govern the alternation of PV and battery energy flows. Finally, authors [20], [21] designed a coordinated controller system to improve the stability of load power by controlling multiple battery units. In this method, battery charging is carried out separately using a PV array, so that optimal battery.

Based on previous studies on PV and battery output monitoring, this article proposes a monitoring design using NodeMCU ESP8266 + INA219, focusing on real-time monitoring, and used to regulate the pump power requirements.

2. METHOD

In a modelling of the monitoring system, it can be done on a PV equipped with a monitoring controller. Figure 1 shows a block diagram of the monitoring system model consisting of a disconnection system, a power supply section consisting of a charging circuit, an energy storage device (EBS), and a DC-DC converter, a measurement circuit, wireless communication, and a microcontroller (MC). In the model, the PV panel terminals (P+ and P−) are connected to the sensor, while the sensor terminals (S− and S+) are connected to adjacent panels of the circuit. The PV panel is separated from the circuit by a controlled electronic switch connected between the P− and S+ nodes. The P− node is the sensor's electrical reference because it always shows the lowest point in the entire circuit. The experimental steps are in accordance with the algorithm. In the initial stage, the monitoring system was designed and programmed, followed by testing and data collection on the water pump load. The hardware design used Proteus.

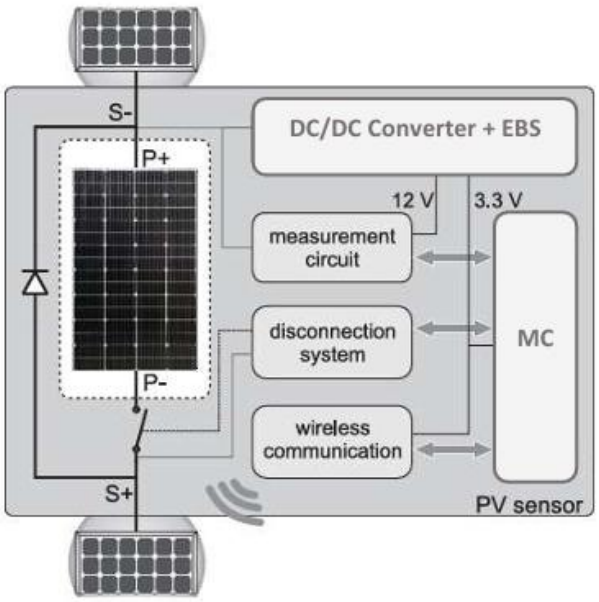

Figure 1. Monitoring circuit model.

2.1 Disconnection Mode

The sensor disconnects the individual panels by utilizing the aforementioned switch and a bypass diode called D in parallel with the branch that includes the panel and the switch, as shown in Figures 1 and 2. The switch blocks the flow of current through the panel, while the bypass diode provides an alternative path for the current of the string I_{String}, thus preventing the interruption of energy generation. The switch is realized with a power Mosfed called M1, whose driving network is depicted in Figure 2.

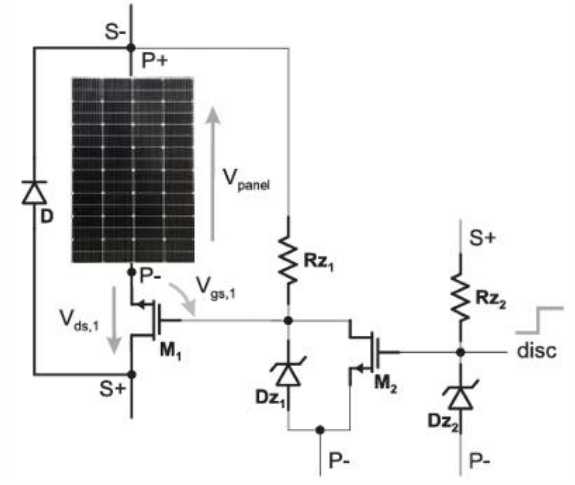

Figure 2. Disconnection Mode.

Figure 3 shows the behavior of the system under three common operating conditions. In particular, Figure 3(a) illustrates the normal operating mode. In this case, the panel is under full irradiation and is conducting the entire I_{String}. Most likely the PV is operating close to its MPP, thus keeping D reverse biased. The panel voltage is high enough to force the Zener diode Dz1 shown in Figure 1 to conduct at its breakdown voltage

ISSN: 2715-6427

(4.7 V), thus making M1 operate in the on state with negligible voltage drop (Rds, ON is about 5 mΩ). The voltage drop VS− S+ dropped across the sensor terminals can be estimated by graphical construction showing the I–V curves of M1 and the panel for the three conditions mentioned earlier. During normal operation, the operating point of M1, corresponding to the current I_{String}, is very close to the y-axis, and VS− S+ (shown by the double arrow line) is almost equal to the operating voltage V_{panel}, thus proving that the sensor does not change the behavior of the panel. Figure 3(b) illustrates the system in a mismatch condition, when the panel is less irradiated than the other panels in the circuit (e.g. due to panel damage, panel aging, or other undesirable objects on the panel surface) and the bypass diode conducts the portion of the circuit I that can no longer flow through the panel. The behavior of the panel is further described by the I–V curves showing a lower photogenerated current. This current flows through M1 as well, so that the gate–source voltage Vgs,1 (see Figure 2) decreases to about 2–3 V corresponding to the new drain current, and the I–V characteristic of M1 is lowered; furthermore, Figure 2 shows that the drain–source voltage Vds,1 coincides with the panel V (neglecting the forward voltage across the bypass diode D). This means that when the bypass condition occurs, the operating point is given by the intersection of the two I–V curves.

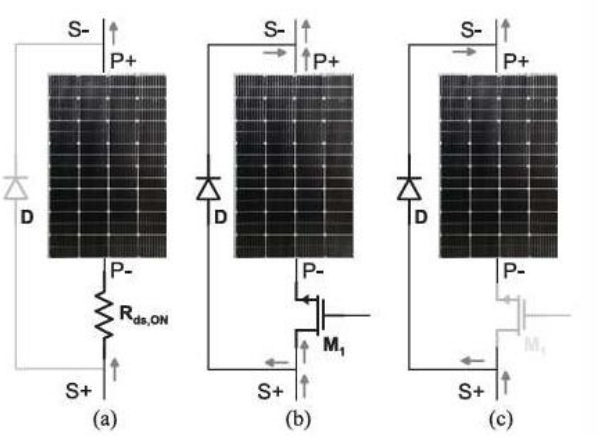

Figure 3. Operation mode (a) normal (b) bypass (c) disconnection.

2.2 Power Supply

Each sensor is supplied by a corresponding panel to avoid additional wiring. In particular, the power supply section must be able to operate properly even though the operating point is imposed on the panel by the MPP tracking converter (MPPT). In other words, the sensor's operating area must cover the entire I–V curve for a wide range of temperature and irradiance levels, even in partial shade conditions (in a panel consisting of three subpanels, the MPP can be placed at about one third of the nominal voltage of the V_{MPP}). In addition, the sensor must be powered by the power supply section during the measurement phase (when the panel is isolated) to guarantee high accuracy in I_{sc} and V_{oc}. detection.

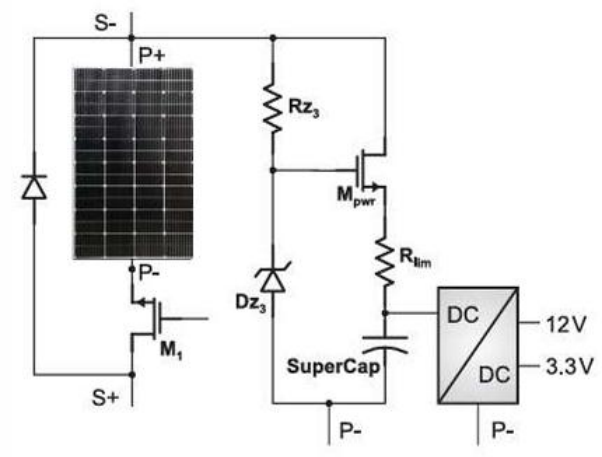

Figure 4. Power supply for monitoring.

As shown in Figure 4, the power supply section consists of two stages. The first stage, which is directly connected to the panel terminals, is a voltage regulator that provides the appropriate voltage level for the EBS

and provides energy for the second stage. The voltage regulator consists of Rz3, Dz3, and Mpwr, while the EBS is a 2F supercapacitor denoted as SuperCap. The Rz3/Dz3 driver network is designed to charge the SuperCap to a voltage level of about 3 V, the charging voltage is limited by the threshold of Dz3 (4.7 V), the gate-source voltage of Mpwr (typically 1.5 V), and the voltage drop across the 10-Ω resistor R_{lim}. When the sensor is turned on (the EBS is fully discharged), R_{lim} limits the charging current to 300 mA, thereby preventing Mpwr from overheating.

2.3 Measurement Section

The sensor performs the identification of the actual operating point through the measurement of V_{panel} and I_{panel}. As is known, the operating point mainly depends on the environmental conditions (temperature and radiation level) and on the MPPT. A correct identification provides information on the actual PV power produced and allows to achieve an accurate power mapping. No information can be obtained on the potentially produced power and the condition of the panel. In order to obtain a complete characterization that is not affected by the actions of the converter, in the second phase the proposed sensor keeps the panel in disconnection mode and measures V_{OC} and I_{SC}. It should be noted that, in normal operation, V_{OC} mainly depends on the temperature, while I_{SC} is proportional to the radiation level. Furthermore, the product of both is proportional to the potentially produced power. However, it should be noted that the measured data cannot directly lead to the local radiation level and temperature related to each subpanel. Although better results can be achieved by performing V_{OC} and I_{SC} measurements on each subpanel, this approach is not suitable for commercial panels because the subpanel electrical terminals are physically connected in series, thus not allowing the insertion of sensors.

2.4 Monitoring system design

Figure 5 shows a block diagram of the PV and battery monitoring system design. This study aims to monitor the voltage, current and power generated by solar panels and batteries. This monitoring uses a microcontroller with the Internet of Things. Monitoring data generated by PV and batteries is sent to Google Sheet and displayed on the I2C LCD in real time.

2.4.1 Solar Panels

Solar panels (PV) function to convert the intensity of solar radiation into DC voltage output. The higher the radiation with the right PV position, the optimal voltage and power will be produced. In this study, a monocrystalline PV with a capacity of 100 Wp was used.

2.4.2 Solar Charge Controller (SCC)

SCC in the solar power generation system (PLTS) functions to control the charging from PV to the battery. SCC plays a role in limiting the charging and discharging of energy from the battery. In this study, an SCC with a capacity of 30 A was used, which was calculated based on the Isc of the PV.

2.4.3 Sensor

In this study, the INA219 sensor is used to measure DC voltage, current and power and has an I2C interface, in the form of SCL and SDA and its I2C interface address can be changed up to 16 addresses. The INA219 sensor can be paralleled to up to 16 addresses with very good measurement accuracy at approximately 0.5%. This high-precision sensor also benefits from 12-bit resolution. The maximum expected bus voltage has a standard value of 32 V. The maximum expected current with a standard value of 3.2 A. The shunt resistance on the sensor has a standard value of 0.01 Ω.

2.4.4 Battery

To store electrical energy in this study, a VRLA battery with a capacity of 100 Ah was used. The battery works by storing energy generated by PV from PLTS. When PV produces more energy than needed, the battery will charge the energy. When PV does not produce electrical energy, the battery will be discharged from the energy that has been stored or used at night. This battery is used at the right time with the settings from the SCC.

2.4.5 Microcontroller (MC)

For the controller in this monitoring system, the NodeMCU ESP8266 microcontroller is used. This microcontroller is equipped with a Wi-Fi network connection between the microcontroller itself and the Wi-Fi network. This microcontroller allows devices to connect directly to a Wi-Fi network and communicate via the TCP/IP protocol. With its small size and low power consumption, the ESP8266 is ideal for IoT applications

ISSN: 2715-6427

that require wireless connectivity. NodeMCU is basically a development of the ESP 8266 with e-Lua-based firmware.

2.4.6 Google Sheet

Google Sheets is a web-based software developed by Google to create tables, simple calculations, and data processing. The difference with working in Microsoft Excel is that Google Sheets allows multiple users to collaborate online on a single worksheet. Google Spreadsheets is an online website application that allows users to create, update, modify worksheets, and share data online in real time. But unlike other spreadsheets, Google Sheets also allows geographically dispersed users to come together on spreadsheets and chat simultaneously using an integrated instant messaging program. Users can upload worksheets directly from their computers or mobile devices, applications like this automatically save any changes, and users can immediately see changes made by others.

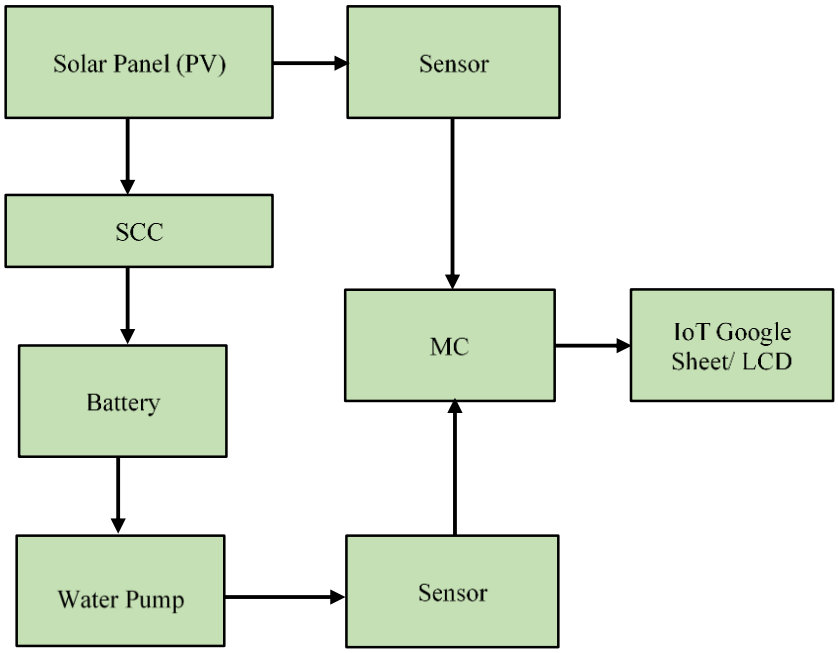

Figure 5. Monitoring system design.

3. RESULTS AND DISCUSSION

The results of the research in this article are the results of testing and analyzing data obtained from the Internet of Things (IoT)-based monitoring system for voltage, current, PV output power and batteries.

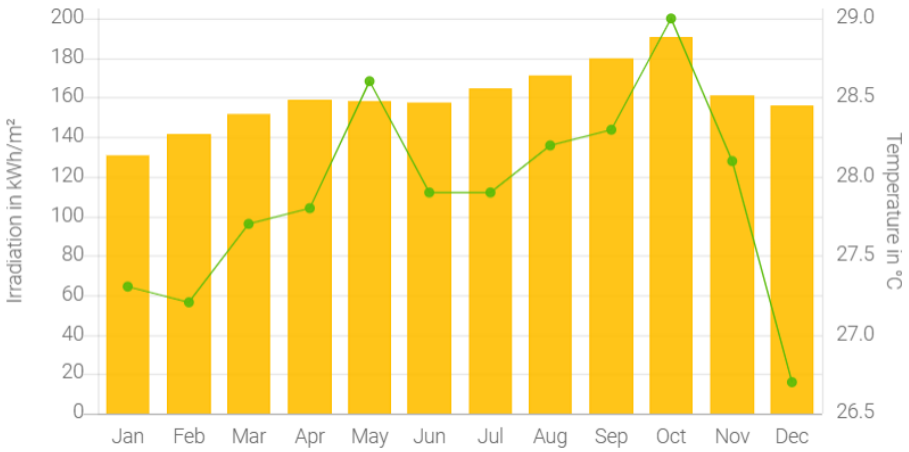

Figure 6. Prediction of solar radiation intensity in 2025.

The research is located at the Sekaran Gunung Pati location in Semarang city which has a latitude coordinate of -07.0502 ° N, 110.398992 ° E. At this location, the annual global radiation is 1920.7 kWh / m² at a

temperature of 28 ° C. Figure 6 shows the predicted intensity of solar radiation in a year. The highest intensity occurs in October and the lowest occurs in January. Based on Figure 6, the radiation potential at the research location is quite large, so it is very appropriate to use PLTS. This study resulted in monitoring of PV and battery output for 3 months, namely from March to May 2025, while Figure 7 shows the preparation for testing in the field by testing the equipment to be used. Figure 8 shows the solar azimuth indicating the angle at the horizontal position towards the north at the research location. This image shows the geographical conditions of the research location, with the aim of determining the potential PV output. Solar azimuth information is intended for PV installation according to solar radiation.

Figure 7. Testing monitoring tools.

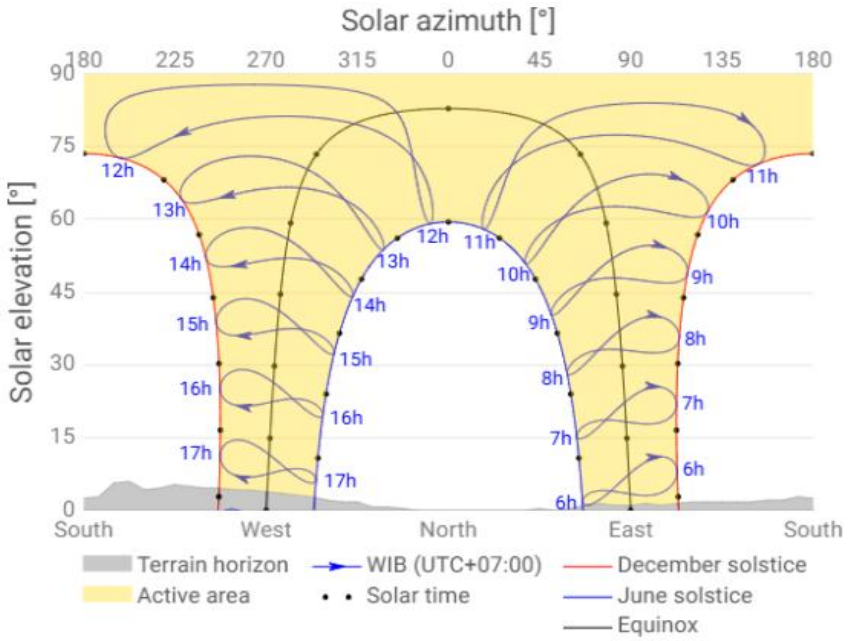

Figure 8. Solar azimuth.

This study was conducted for 12 weeks or 3 months. PV and battery monitoring in the first week of the first month can be seen in Figure 9, while Figure 10 shows PV and battery monitoring in the first week of the

ISSN: 2715-6427

second month. The results of PV monitoring in the first week of the first and second months showed that the PV output voltage ranged from 12 to 13 V DC. This shows that the research location has the same radiation for 2 months, while the output current and power depend on the load consumption.

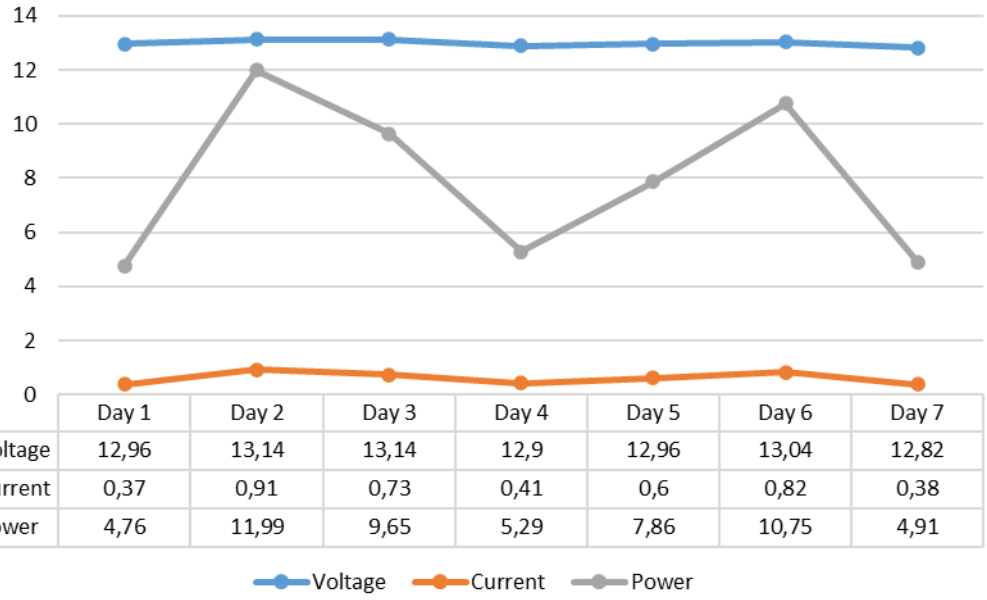

	Day 1	Day 2	Day 3	Day 4	Day 5	Day 6	Day 7
Voltage	12,96	13,14	13,14	12,9	12,96	13,04	12,82
Current	0,37	0,91	0,73	0,41	0,6	0,82	0,38
Power	4,76	11,99	9,65	5,29	7,86	10,75	4,91

Figure 9. PV monitoring data for the first week of the first month.

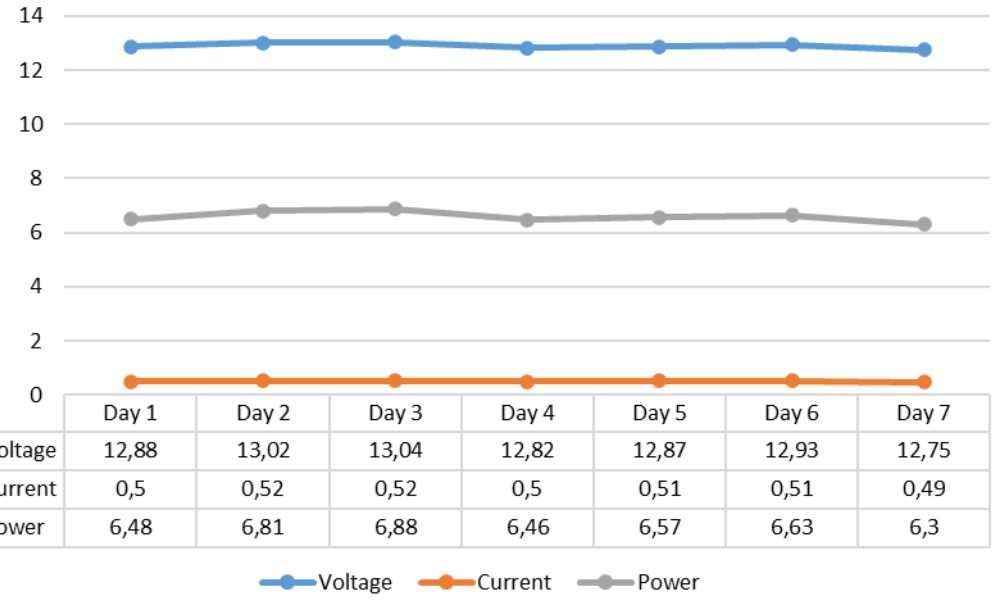

	Day 1	Day 2	Day 3	Day 4	Day 5	Day 6	Day 7
Voltage	12,88	13,02	13,04	12,82	12,87	12,93	12,75
Current	0,5	0,52	0,52	0,5	0,51	0,51	0,49
Power	6,48	6,81	6,88	6,46	6,57	6,63	6,3

Figure 10. Battery monitoring data for the first week of the first month.

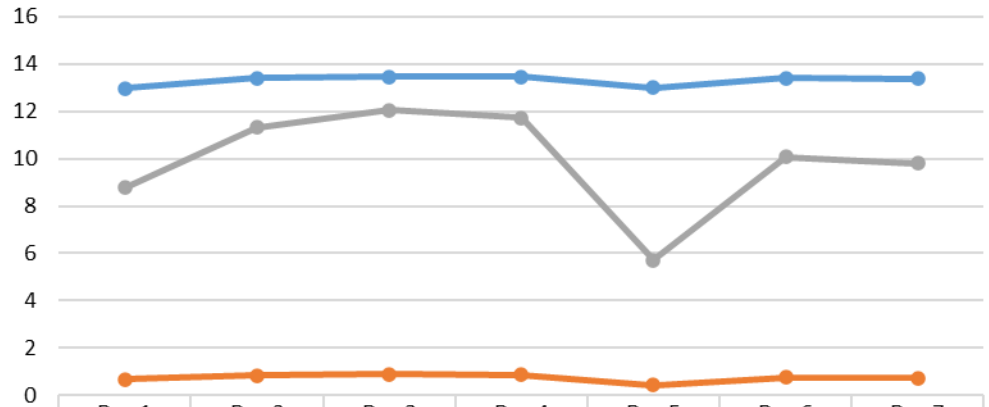

	Day 1	Day 2	Day 3	Day 4	Day 5	Day 6	Day 7
Voltage	12,97	13,4	13,45	13,45	13	13,4	13,38
Current	0,66	0,84	0,89	0,87	0,43	0,75	0,73
Power	8,78	11,31	12,06	11,74	5,7	10,07	9,81

Figure 11. PV monitoring data for the first week of the second month.

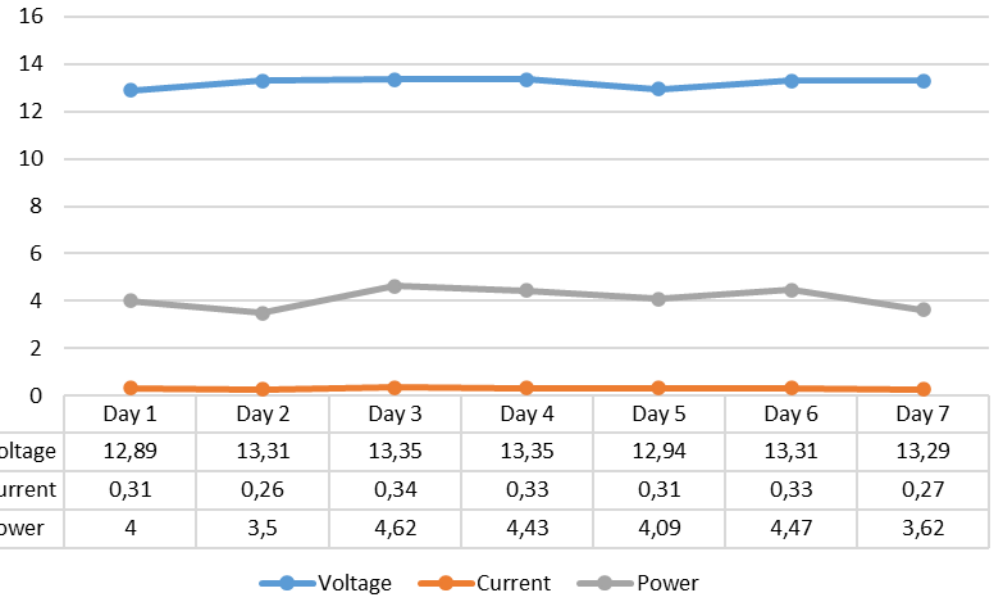

	Day 1	Day 2	Day 3	Day 4	Day 5	Day 6	Day 7
Voltage	12,89	13,31	13,35	13,35	12,94	13,31	13,29
Current	0,31	0,26	0,34	0,33	0,31	0,33	0,27
Power	4	3,5	4,62	4,43	4,09	4,47	3,62

Figure 12. Battery monitoring data for the first week of the second month.

The PV contribution to power is calculated as the product of the measured Voc and Isc weighted by the filling factor, which is then obtained from the nominal values reported in the data sheet through temperature adjustment. Under uniform irradiance and temperature conditions, the PV curves will coincide. In case of mismatch, the power loss due to mismatch is measured based on the gap between the maximum power that can be produced and that estimated by the iMPPT algorithm, while the decrease between the latter and the measured represents the power loss caused by MPPT failure. Initially the weather conditions are completely clear, then the power that the PV can produce gradually decreases due to the module effect. Then the MPPT algorithm forces the PV voltage to increase assuming uniform conditions. This analysis allows a detailed quantification of the voltage, current and power outputs, thus supporting an easy comparison between investment and maintenance actions. It is worth highlighting the power drop due to SCC failure, which can be avoided by using the appropriate on-demand MPPT offered by the sensors. In particular, the PV that limits the power production,

ISSN: 2715-6427

due to the PV having a lower Isc than the estimated IMPP, can be disconnected quickly. This causes a local maximum drop located at a voltage higher than the VMPP and the PV will approach the global MPP.

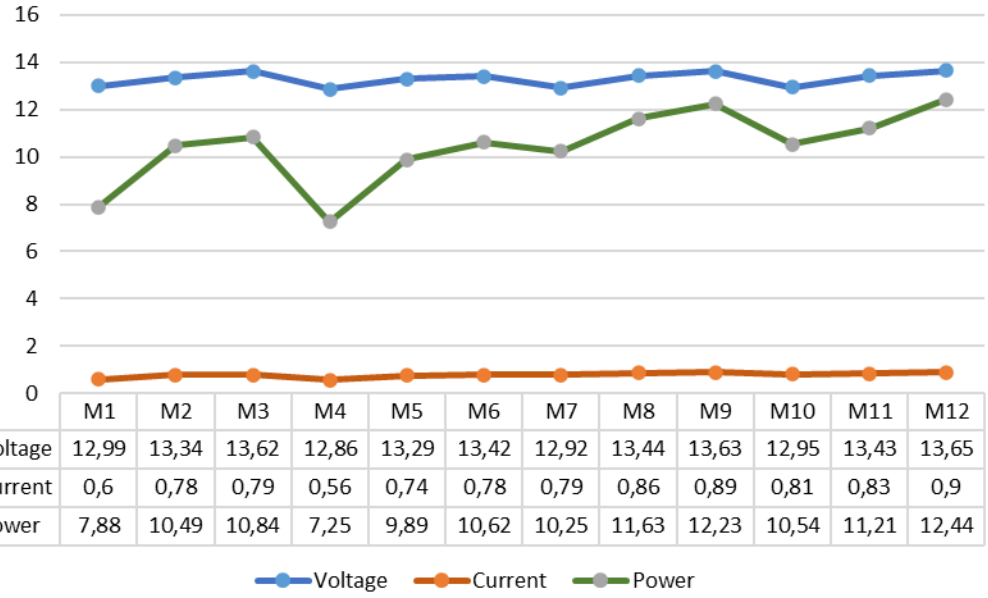

	M1	M2	M3	M4	M5	M6	M7	M8	M9	M10	M11	M12
Voltage	12,99	13,34	13,62	12,86	13,29	13,42	12,92	13,44	13,63	12,95	13,43	13,65
Current	0,6	0,78	0,79	0,56	0,74	0,78	0,79	0,86	0,89	0,81	0,83	0,9
Power	7,88	10,49	10,84	7,25	9,89	10,62	10,25	11,63	12,23	10,54	11,21	12,44

Figure 13. PV monitoring data for 3 months or 12 weeks.

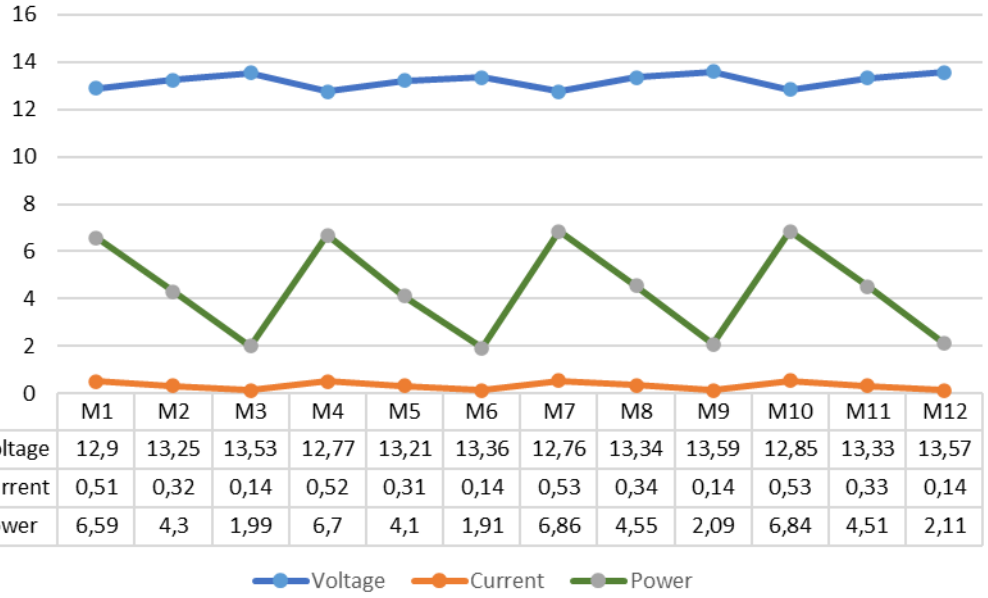

	M1	M2	M3	M4	M5	M6	M7	M8	M9	M10	M11	M12
Voltage	12,9	13,25	13,53	12,77	13,21	13,36	12,76	13,34	13,59	12,85	13,33	13,57
Current	0,51	0,32	0,14	0,52	0,31	0,14	0,53	0,34	0,14	0,53	0,33	0,14
Power	6,59	4,3	1,99	6,7	4,1	1,91	6,86	4,55	2,09	6,84	4,51	2,11

Figure 14. Battery monitoring data for 3 months or 12 weeks.

The research that has been carried out is able to perform a monitoring system on the output of solar panels (PV) and batteries. Experimental investigations that have been carried out to verify the effectiveness of the proposed monitoring system have been shown by the results of monitoring on PV and batteries. The monitoring system is able to perform measurements well for 3 months. The results of monitoring measurements in this study are also influenced by the intensity of solar radiation.

4. CONCLUSION

The research conducted was able to run a monitoring system on the output of solar panels (PV) and batteries based on the Internet of Things using the INA219 sensor with an I2C LCD display in real-time. The sensor is suitable for measuring various key research parameters and actual operating points without affecting

energy production. In addition, the sensor showed good performance even in bypass conditions. The monitoring system was able to perform good measurements for 3 months. The results of the monitoring measurements in this study were also influenced by the intensity of solar radiation. This research can be developed to monitor the load, with a fuzzy logic controller. The monitored load is not only the AC load but also the DC load.

ACKNOWLEDGEMENTS

We would like to thank the Lembaga Penelitian dan Pengabdian Masyarakat (LPPM) of Universitas Negeri Semarang for providing financial support for the implementation of research in the field of renewable energy monitoring.

REFERENCES

[1] J. Han, I. Lee, and S. H. Kim, "User-friendly monitoring system for residential PV system based on low-cost power line communication," *IEEE Trans. Consum. Electron.*, vol. 61, no. 2, pp. 175–180, 2015, doi: 10.1109/TCE.2015.7150571.

[2] H. Mortazavi, H. Mehrjerdi, M. Saad, S. Lefebvre, D. Asber, and L. Lenoir, "A Monitoring Technique for Reversed Power Flow Detection with High PV Penetration Level," *IEEE Trans. Smart Grid*, vol. 6, no. 5, pp. 2221–2232, 2015, doi: 10.1109/TSG.2015.2397887.

[3] W. Mao, X. Zhang, R. Cao, F. Wang, T. Zhao, and L. Xu, "A research on power line communication based on parallel resonant coupling technology in pv module monitoring," *IEEE Trans. Ind. Electron.*, vol. 65, no. 3, pp. 2653–2662, 2018, doi: 10.1109/TIE.2017.2736483.

[4] N. Agarwal, A. Arya, M. W. Ahmad, and S. Anand, "Lifetime Monitoring of Electrolytic Capacitor to Maximize Earnings from Grid-Feeding PV System," *IEEE Trans. Ind. Electron.*, vol. 63, no. 11, pp. 7049–7058, 2016, doi: 10.1109/TIE.2016.2586020.

[5] P. Guerriero, F. Di Napoli, G. Vallone, V. Dalessandro, and S. Daliento, "Monitoring and diagnostics of PV plants by a wireless self-powered sensor for individual panels," *IEEE J. Photovoltaics*, vol. 6, no. 1, pp. 286–294, 2016, doi: 10.1109/JPHOTOV.2015.2484961.

[6] L. G. Monteiro *et al.*, "Field I-V Curve Measurements Methodology at String Level to Monitor Failures and the Degradation Process: A Case Study of a 1.42 MWp PV Power Plant," *IEEE Access*, vol. 8, pp. 226845–226865, 2020, doi: 10.1109/ACCESS.2020.3044832.

[7] Å. Skomedal, H. Haug, and E. S. Marstein, "Endogenous Soiling Rate Determination and Detection of Cleaning Events in Utility-Scale PV Plants," *IEEE J. Photovoltaics*, vol. 9, no. 3, pp. 858–863, 2019, doi: 10.1109/JPHOTOV.2019.2899741.

[8] M. W. Ahmad, N. Agarwal, and S. Anand, "Online Monitoring Technique for Aluminum Electrolytic Capacitor in Solar PV-Based DC System," *IEEE Trans. Ind. Electron.*, vol. 63, no. 11, pp. 7059–7066, 2016, doi: 10.1109/TIE.2016.2582470.

[9] M. G. Deceglie, T. J. Silverman, B. Marion, and S. R. Kurtz, "Real-Time Series Resistance Monitoring in PV Systems Without the Need for I-V Curves," *IEEE J. Photovoltaics*, vol. 5, no. 6, pp. 1706–1709, 2015, doi: 10.1109/JPHOTOV.2015.2478070.

[10] G. Di Lorenzo, R. Araneo, M. Mitolo, A. Niccolai, and F. Grimaccia, "Review of O&M Practices in PV Plants: Failures, Solutions, Remote Control, and Monitoring Tools," *IEEE J. Photovoltaics*, vol. 10, no. 4, pp. 914–926, 2020, doi: 10.1109/JPHOTOV.2020.2994531.

[11] N. Agarwal, M. W. Ahmad, and S. Anand, "Quasi-Online Technique for Health Monitoring of Capacitor in Single-Phase Solar Inverter," *IEEE Trans. Power Electron.*, vol. 33, no. 6, pp. 5283–5291, 2018, doi: 10.1109/TPEL.2017.2736162.

[12] J. Slapšak, S. Mitterhofer, M. Topic, and M. Jankovec, "Wireless System for in Situ Monitoring of Moisture Ingress in PV Modules," *IEEE J. Photovoltaics*, vol. 9, no. 5, pp. 1316–1323, 2019, doi: 10.1109/JPHOTOV.2019.2918044.

[13] Z. Zhao, H. Hu, Z. He, H. H. C. Iu, P. Davari, and F. Blaabjerg, "Power Electronics-Based Safety Enhancement Technologies for Lithium-Ion Batteries: An Overview From Battery Management Perspective," *IEEE Trans. Power Electron.*, vol. 38, no. 7, pp. 8922–8955, 2023, doi: 10.1109/TPEL.2023.3265278.

[14] S. Jafari and Y. C. Byun, "Prediction of the Battery State Using the Digital Twin Framework Based on the Battery Management System," *IEEE Access*, vol. 10, no. December, pp. 124685–124696, 2022, doi: 10.1109/ACCESS.2022.3225093.

[15] B. G. Carkhuff, P. A. Demirev, and R. Srinivasan, "Impedance-Based Battery Management System for Safety Monitoring of Lithium-Ion Batteries," *IEEE Trans. Ind. Electron.*, vol. 65, no. 8, pp. 6497–6504, 2018, doi: 10.1109/TIE.2017.2786199.

[16] S. Yang and S. Zhang, "Energy Balance Control of Multi Group Lithium Ion Batteries Under Internet of Things Technology," *IEEE Access*, vol. 12, no. July, pp. 102784–102797, 2024, doi: 10.1109/ACCESS.2024.3430318.

[17] A. Kusmantoro, "Real-Time Microgrid For Submersible Pump Energy Consumption Based On Fuzzy Logic Controller", International Conference on Advanced Mechatronics, Intelligent Manufacture and Industrial Automation (ICAMIMIA), pp. 948 – 953, 2024, doi: 10.1109/ICAMIMIA60881.2023.10427800.

[18] A. Kusmantoro, "Power Regulation on PV and Grid With Monitoring Load Power in Residential", 11th International Conference on Electrical Engineering, Computer Science and Informatics (EECSI), pp. 118 – 123, 2024, doi: 10.1109/EECSI63442.2024.10776067.

[19] A. Kusmantoro, ""Multi-Inverter Coordinated Control on AC Microgrid for Increased Load Power", Sixth International Conference on Vocational Education and Electrical Engineering (ICVEE), pp. 90 – 95, 2023, doi: 10.1109/ICVEE59738.2023.10348326.

[20] A. Kusmantoro and I. Farikhah, "Solar power and multi-battery for new configuration DC microgrid using centralized control," *Arch. Electr. Eng.*, vol. 72, no. 4, pp. 931–950, 2023, doi: 10.24425/aee.2023.147419.

[21] A. Kusmantoro, A. Priyadi, V. L. Budiharto Putri, and M. Hery Purnomo, "Coordinated Control of Battery Energy Storage System Based on Fuzzy Logic for Microgrid with Modified AC Coupling Configuration," *Int. J. Intell. Eng. Syst.*, vol. 14, no. 2, pp. 495–510, 2021, doi: 10.22266/ijies2021.0430.45.